

Article

A Parametric Optimized Method for Three-Dimensional Corner Joints in Wooden Furniture

Xiutong Xu ¹ , Xianqing Xiong ^{1,2,*}, Xinyi Yue ¹ and Mei Zhang ¹

¹ College of Furnishings and Industrial Design, Nanjing Forestry University, Nanjing 210037, China; xiutongxu@njfu.edu.cn (X.X.); yuexinyi0331@163.com (X.Y.); zhangmei@njfu.edu.cn (M.Z.)

² Co-Innovation Center of Efficient Processing and Utilization of Forest Resources, Nanjing Forestry University, Nanjing 210037, China

* Correspondence: xiongqianqing@njfu.edu.cn

Abstract: The three-dimensional corner joint is a type of joint in wooden furniture structures with complex parameter relationships and many constraints. Traditional furniture structure design requires repeated modifications of geometric models to determine parameter dimensions, which is inefficient and challenging and severely impacts the development of the digital design and manufacture process. Based on the ideal value range of mortise–tenon joints, this study derived a parametric optimized method of three-dimensional corner joints in wooden furniture and refined the theoretical value range of at least four main parameters: the width of the beneficial mortise (B_2), the depth of the cede mortise (C_1), the margin thickness from the cede tenon to the rail₁ reference edge (b_{t1}), and the margin thickness from the beneficial tenon to the rail₂ reference edge (b_{t2}). With case verification, the results show that in the axial direction of the cede tenon, the $maxC_1$ decreased by 5.4 mm and the combination of (B_2, C_1) reduced at least 23 kinds. In the cases of different post widths and the margin thickness from rail₂'s reference edge to the post's reference edge (B_{tm2}), the value range and value quantity of b_{t2} were narrowed and decreased in various degrees. In the axial direction of the beneficial tenon, the value range and quantity of available values of the margin thickness from the cede tenon to the rail₁ reference edge (b_{t1}) decrease with decreasing margin thickness from the rail₁ reference edge to the post reference edge (B_{tm1}) when B_{tm1} is less than constant z . The parametric optimized method of three-dimensional corner joints in wooden furniture can effectively reduce the parameter dimensional value range, both theoretically and practically, and more refined value ranges can be obtained by setting more standard values. This method also provides ideas for the digital and standardized design of wooden furniture structures.

Keywords: wooden furniture; mortise–tenon joints; three-dimension corner joints; parametric method; dimension value determination



Citation: Xu, X.; Xiong, X.; Yue, X.; Zhang, M. A Parametric Optimized Method for Three-Dimensional Corner Joints in Wooden Furniture. *Forests* **2023**, *14*, 1063. <https://doi.org/10.3390/f14051063>

Academic Editors: Ioannis A. Barboutis and Vasiliki Kamperidou

Received: 8 April 2023
Revised: 19 May 2023
Accepted: 19 May 2023
Published: 22 May 2023



Copyright: © 2023 by the authors. Licensee MDPI, Basel, Switzerland. This article is an open access article distributed under the terms and conditions of the Creative Commons Attribution (CC BY) license (<https://creativecommons.org/licenses/by/4.0/>).

1. Introduction

With the development of industrial technology and the improvement of digitization and informatization levels, digital and intelligent technologies have developed rapidly in recent years and have been widely applied in the design, manufacturing, and marketing of wooden furniture, effectively improving product quality and production efficiency [1–4]. Among them, the parametric design method has been widely used in the entire process of wooden furniture design and manufacturing and has initially solved the connection problem between the design and manufacturing ends through Computer-Aided Design, Computer-Aided Process Planning and Computer-Aided Manufacturing (CAD/CAPP/CAM). In addition, with the help of Computer-Aided Design and Computer-Aided Engineering (CAD/CAE), structural performance testing can be conducted without physical mechanical tests, which promotes the design efficiency and production of wooden furniture [5–8].

Mortise–tenon joints are often used for wooden furniture assembly. Currently, the design and processing workflow for mortise–tenon joints in most Chinese enterprises is roughly as follows: First, make drawings and 3D models based on parts' dimensions. Then, the mortise–tenon joint dimensions are designed according to each part's width and thickness and added to the drawing and 3D model. Finally, the dimensions are transformed into processing code through the Computer Numerical Control (CNC) machining program, and the code is sent to the CNC machine tool for processing [9,10]. In the case of the diverse types, complex structures, and variable dimensions of mortise–tenon joints, relying solely on ideal traditional design methods will result in a large amount of repetitive work. At the same time, there are no standard dimensions for mortise–tenon joints. The unreasonable mortise–tenon joints parameter dimensions determination method seriously affects the digital production efficiency and quality of wooden furniture structures [11,12].

Using a parametric design method to determine joint dimensions is an effective way to improve standardization, which should be based on good properties, high processing efficiency, and convenient, fast design [13–15]. Kasal et al. [16] and Hu et al. [17] studied the influence of the dimensions of round-end mortise–tenon joints on mechanical properties. Guan [18] and Smardzewski [19] proposed a rapid calculation method for mechanical properties based on different dimensions of mortise–tenon joints, which can be used as a reference for production technicians and effectively improve the standardization of wooden furniture structure design. Tang et al. [20] developed an intelligent design and processing code for mortise–tenon joints, which can automatically generate Numerical Control (NC) codes that meet processing requirements based on determined joint dimensions, achieving the preliminary connection of mortise–tenon joint dimensions and NC processing programs. In addition, many optimized methods can be applied to the standardization of furniture structures, such as Group Technology, Parametric Design, Cluster Analysis, Experiment, Finite Element Method, Response Surface Methodology, etc., all of which provide some theoretical and practical bases on the optimization for structure parameters in wooden furniture [7,12,17,21].

Three-dimensional corner joints in wooden furniture are one of the most challenging joints in furniture structure design due to their small dimension and potential for structure conflicts [22]. Typically, a three-dimensional corner joint consists of a post and two perpendicular rails, which are connected by rectangular or round-end tenons. The direction with higher properties requirements uses a beneficial tenon, while the other rail uses a cede tenon, which sacrifices the cede tenon's length for the beneficial tenon's thickness. If ideal calculation methods are used to determine the parameter dimension values and value ranges, there might be structural conflicts. Furthermore, because wooden furniture components vary greatly in dimensions and shapes, adjusting even one value in the joint can result in a complete redesign of the entire structure [23]. Therefore, in this situation, it is an effective approach to optimize the dimension parameter value range of three-dimensional corner joints based on existing ideal methods. By inputting necessary values, the parameter-covering value ranges can be quickly narrowed down to avoid excessive options and potential conflicts [24,25]. For a better understanding, Figure 1 shows the flowchart of this research.

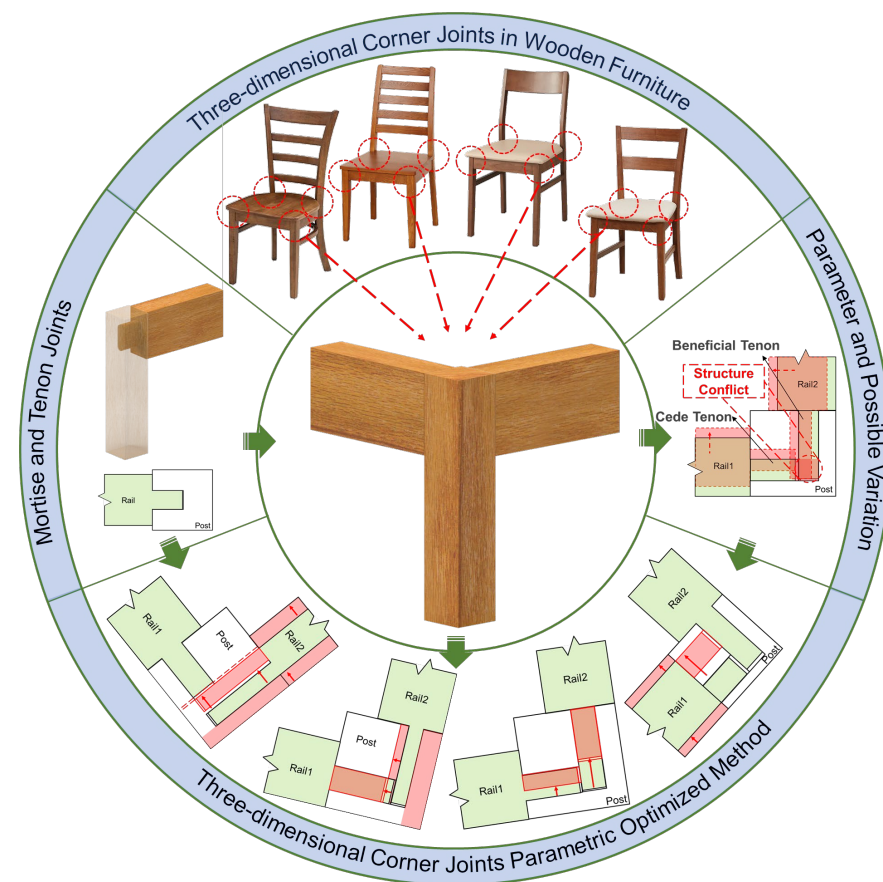


Figure 1. Flowchart.

2. Materials and Methods

2.1. Steps

This research includes three steps. First, according to the parameter value calculation formula of mortise–tenon joints, the ideal value range of each parameter is obtained. Second, an optimized method for the structure of three-dimensional corner joints in wooden furniture was derived based on the correlation between different parameters. Finally, using collected examples of the basic dimensions of three-dimensional corner joints, calculations were performed using the ideal method for determining the basic dimensions covering the value range and the parametric optimized method. Data analysis and comparison will be conducted.

2.2. Three-Dimensional Corner Joints Parameter Value Optimized Method

2.2.1. Mortise–Tenon Joint Parameter Basic Ideal Value Method

According to [26], the dimensions of the mortise and tenon are determined by multiplying a certain coefficient by the rail or the post dimensions. After a simple transformation, the value range obtained by the ideal calculation formula for mortise dimensions is given in Formula (1). In this study, only the case where the tenon width and mortise height of the three-dimensional corner joint are equal is considered, and therefore the height parameter of the mortise is not taken into account.

$$0.3T_t \leq B \leq 0.6T_t \quad (1a)$$

$$0.5 W_m + \Delta C \leq C \leq W_m - z \quad (1b)$$

where T_t is rail thickness; W_m is post width; B, C are mortise width and mortise depth, respectively; ΔC is the fitting parameter of mortise depth and tenon length, which is a redundancy not only to prevent incomplete assembly between tenon and mortise but also a technological gap for glue; z is the fixed value of the safety margin thickness for the drilling operation. The common values of B are 5, 6, 8, 10, 12, 14, 16, 20, etc. W_m can also be replaced by T_m , where T_m is post thickness. All parameter values are in units of mm.

In addition to the mortise parameter dimensions, the rail and the post dimensions and the margin thickness parameter are constrained by requirements such as shape and manufacturing, as shown in Figure 2. Therefore, their basic value ranges can ideally be described as in Formula (2).

$$T_t \leq T_m \tag{2a}$$

$$z \leq B_m \leq T_m - B - z \tag{2b}$$

$$0 \leq b_t \leq T_t - B \tag{2c}$$

$$0 \leq B_{tm} \leq T_m - T_t \tag{2d}$$

where T_t is rail thickness; T_m is post thickness; B is mortise width; z is the fixed value of the safety drilling margin thickness from mortise to post edge; B_m is the margin thickness from mortise to post reference edge; b_t is margin thickness from mortise-tenon to rail reference edge; B_{tm} is margin thickness from the rail reference edge to the post reference edge. The actual values of B_m, B_{tm}, b_t are correlated, and the equation can be described as $B_m = b_t + B_{tm}$. The common values of B are 5, 6, 8, 10, 12, 14, 16, 20, and so on. T_m can also be replaced by W_m , where W_m is post width. $b_t, B_m,$ and B_{tm} are collectively referred to as the margin thickness parameter. All parameter values are in units of mm.

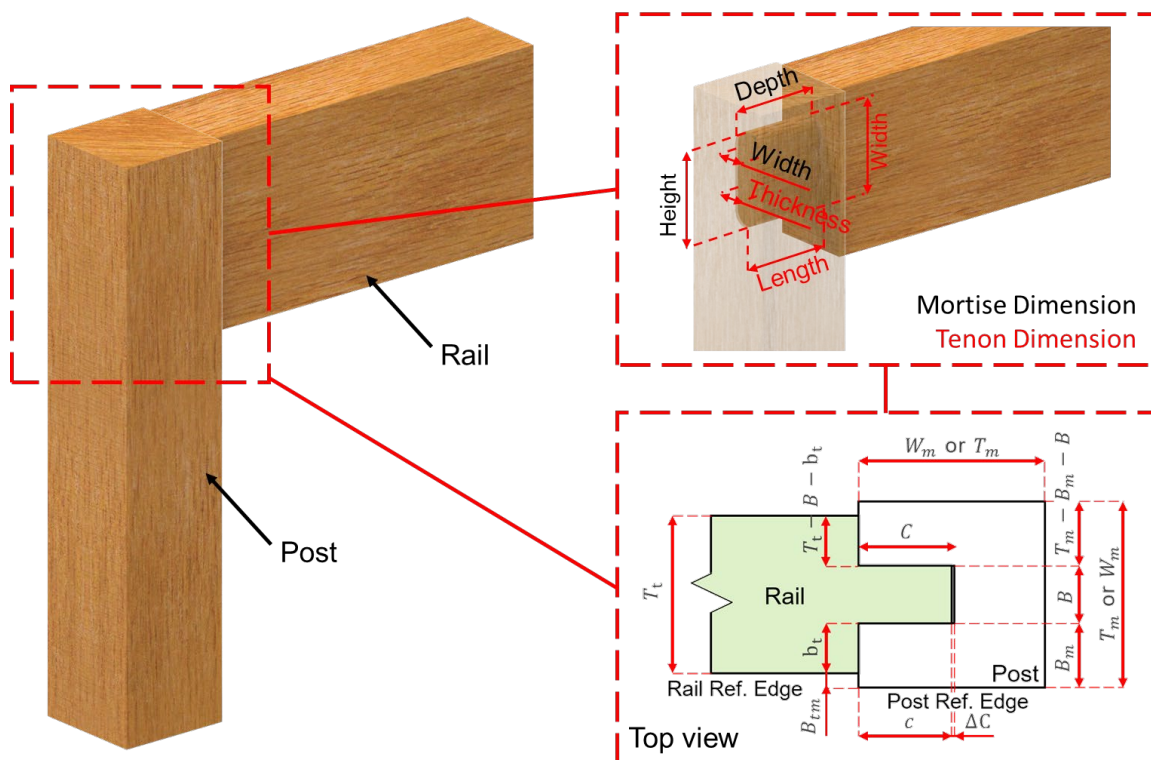


Figure 2. Mortise-tenon joints basic parameters.

Based on Formulas (1) and (2), the parameter values of the three-dimensional corner joint can be further generalized, and the parametric optimized method can be further improved based on its characteristics. Because the constraints of the three-dimensional corner joint are different in the axial direction of the beneficial tenon and the cede tenon, the parameter values for these two directions are optimized, as shown in Figure 3. Generally, the axial direction of the beneficial tenon corresponding to the post reference edge is W_m , while the axial direction of the cede tenon corresponding to the post reference edge is T_m .

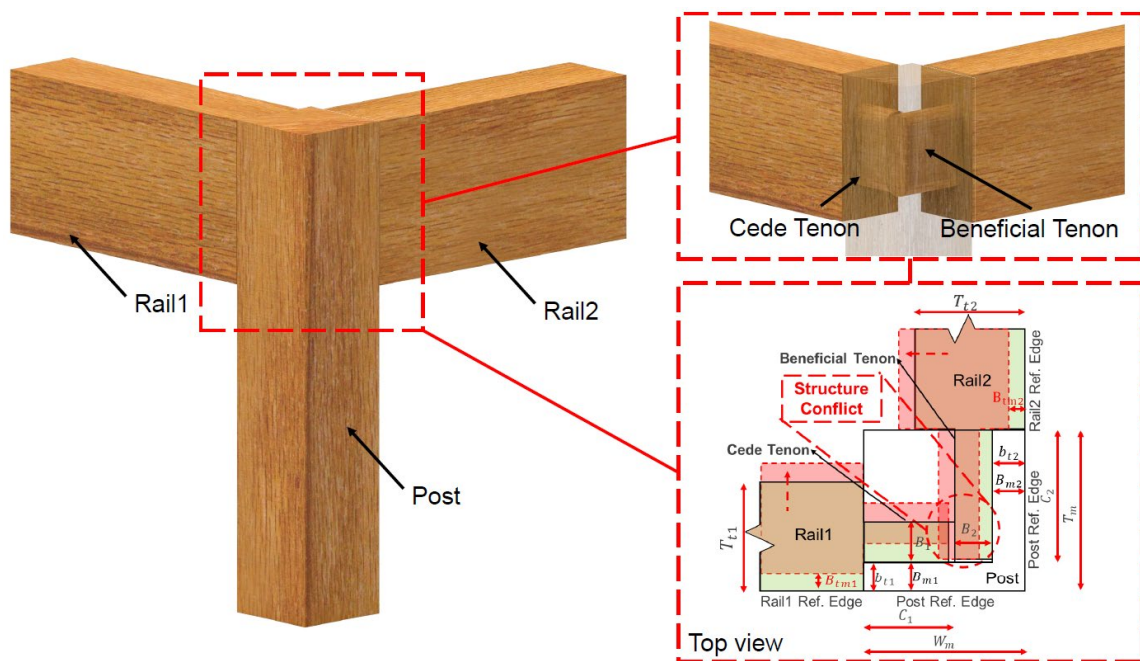


Figure 3. Parameters and possible variations in dimension and relative position of three-dimensional corner joints. The green part refers to the situation where the rail reference edge is flush with the post reference edge, while the red part refers to the situation where two rails or tenons move inward.

2.2.2. Parametric Optimized Method in the Axial Direction of the Beneficial Tenon

In the axial direction of the beneficial tenon, the depth of the beneficial mortise (C_2), and the width of the cede mortise (B_1) are the same in Formula (1). The margin thickness from the cede mortise to the post reference edge (B_{m1}), and the margin thickness from the rail₁ reference edge to the post reference edge (B_{tm1}) are the same as in Formula (2). As shown in Figure 4, based on the different thicknesses of the rail₁ (T_{t1}) and the post (T_m), the margin thickness from the cede mortise or tenon to the rail₁ reference edge (b_{t1}) can be further optimized for the range of values.

If $T_{t1} < T_m - z$, b_{t1} 's value range equals Formula (2c).

If $T_m - z \leq T_{t1} < T_m$, b_{t1} 's value range can be expressed as

$$z - B_{tm1} \leq b_{t1} \leq T_m - B_1 - z - B_{tm1} \tag{3a}$$

If $T_{t1} = T_m$, b_{t1} 's value range can be expressed as

$$z \leq b_{t1} \leq T_m - B_1 - z \tag{3b}$$

where T_{t1} is rail₁ thickness; T_m is post thickness; b_{t1} is margin thickness from cede mortise-tenon to rail₁ reference edge; B_1 is cede mortise width; z is the fixed value of the safety drilling margin thickness from mortise to the post edge. All parameter values are in units of mm. In Formula (3b), T_m can also be replaced by T_t .

2.2.3. Parametric Optimized Method in the Axial Direction of Cede Tenon

In the axial direction of the cede tenon, various dimensional parameters are interdependent, and the depth of the cede mortise (C_1) and the width of the beneficial mortise (B_2) are essential to meet the structural requirements. However, the values of C_1 and B_2 can sometimes be interdependent, and, therefore, the value ranges of C_1 and B_2 are described separately based on the following situations. C_1 's value range can be described as

$$0.5W_m + \Delta C \leq C_1 \leq W_m - B_2 - z \tag{4a}$$

If $0.5W_m - z - \Delta C \geq 0.6T_{t2}$, B_2 's value range can be described as in Formula (1a). Further moreover, if $0.5W_m - z - \Delta C < 0.6T_{t2}$, it can be described as

$$0.3T_{t2} \leq B_2 \leq 0.5W_m - \Delta C - z \tag{4b}$$

The value of margin thickness parameters must be based on the reasonable values of B_2 and C_1 , as shown in Figure 5. The value range of the margin thickness from the beneficial mortise to the post reference edge (B_{m2}) can be described as

$$z \leq B_{m2} \leq W_m - C_1 - B_2 \tag{5a}$$

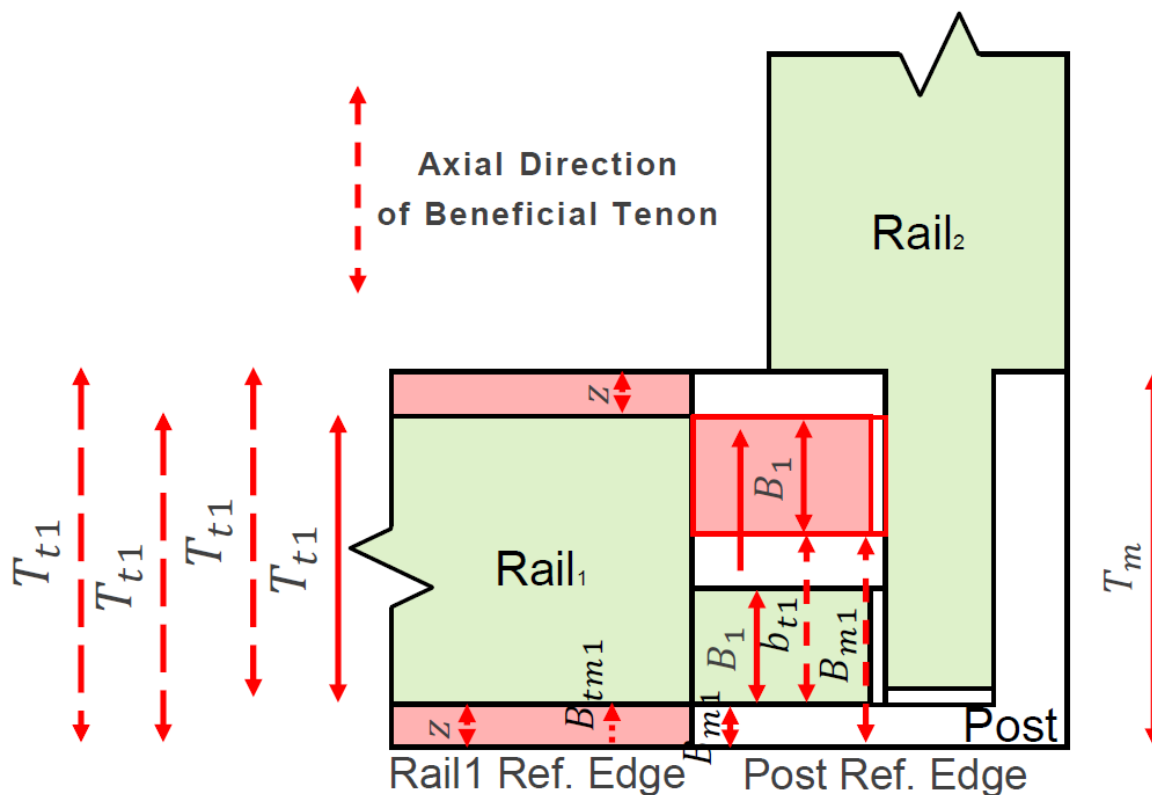


Figure 4. Possible change in margin thickness parameter in the axial direction of the beneficial tenon, where the green part is the general situation, and the red part is the possible change of T_{t1} and margin parameters.

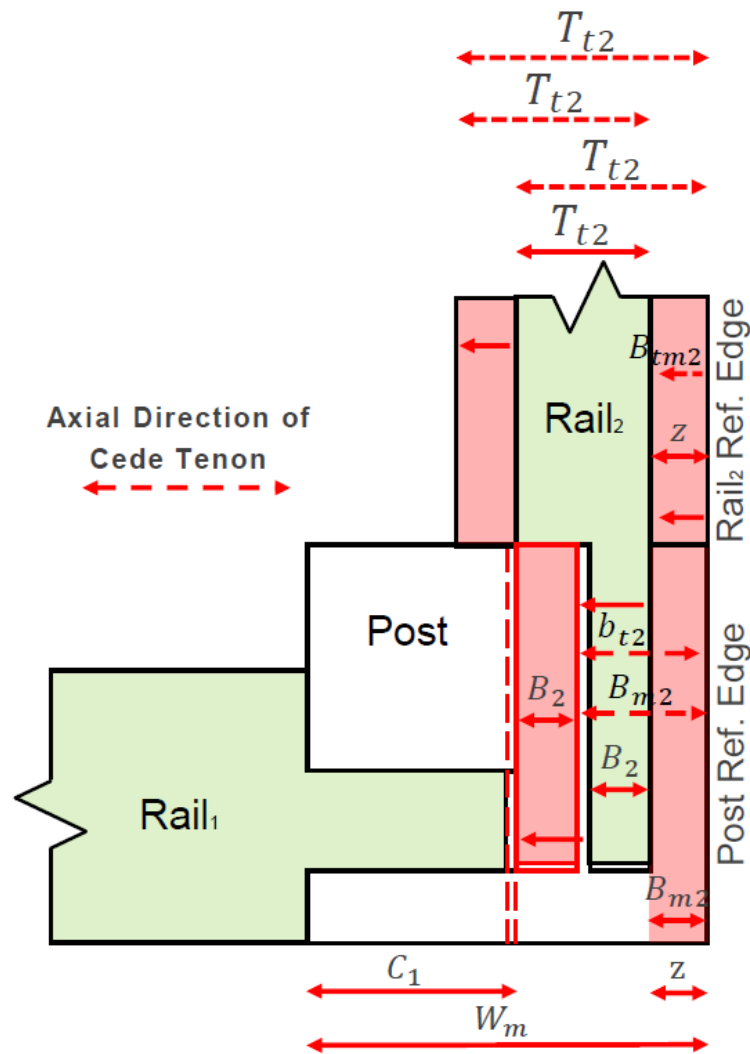


Figure 5. Possible value change of margin thickness parameter in cede tenon axis, where the green part is the general situation, and the red part is the possible change of T_{t2} and margin parameters.

The maximum value of the margin thickness from the rail₂'s reference edge to the post's reference edge ($maxB_{tm2}$) can be further described according to the value range limitation of B_{m2} . B_{tm2} 's value range can be described as

$$0 \leq B_{tm2} \leq W_m - C_1 - B_2 \tag{5b}$$

For the margin thickness parameter from the beneficial tenon to rail₂ reference edge (b_{t2}), the value range can be further refined based on different parameters such as T_{t2} , W_m , C_1 , B_2 , and B_{tm2} .

If $T_{t2} \leq W_m - C_1$ and $0 \leq B_{tm2} \leq W_m - C_1 - T_{t2}$, b_{t2} 's value range equals Formula (2c).

If $T_{t2} \leq W_m - C_1$ and $W_m - C_1 - T_{t2} < B_{tm2} \leq W_m - C_1 - B_2$, b_{t2} 's value range can be written as

$$0 \leq b_{t2} \leq W_m - C_1 - B_2 - B_{tm2} \tag{6a}$$

If $W_m - C_1 < T_{t2}$ and $B_{tm2} = 0$, b_{t2} 's value range can be written as

$$z \leq b_{t2} \leq W_m - C_1 - B_2 \tag{6b}$$

If $W_m - C_1 < T_{t2}$ and $0 < B_{tm2} \leq z$, b_{t2} 's value range can be written as

$$z - B_{tm2} \leq b_{t2} \leq W_m - C_1 - B_2 - B_{tm2} \tag{6c}$$

If $W_m - C_1 < T_{t2}$ and $z < B_{tm2} \leq W_m - C_1 - B_2$, b_{t2} 's value range can be written as

$$0 \leq b_{t2} \leq W_m - C_1 - B_2 - B_{tm2} \quad (6d)$$

where T_{t2} is rail₂ thickness; W_m is post width; B_2 is beneficial mortise width; C_1 is cede mortise depth; ΔC is the fitting parameter of mortise depth and tenon length, which is a redundancy not only to prevent incomplete assembly between tenon and mortise but also a technological gap for glue; z is the fixed value of the safety drilling margin thickness from mortise to the post edge; b_{t2} is margin thickness from beneficial mortise–tenon to rail₂ reference edge; B_{m2} is margin thickness from beneficial mortise to the post reference edge; B_{tm2} is margin thickness from rail₂ reference edge to post reference edge. All parameter values are in units of mm.

2.3. Cases' Basic Dimension Acquisition and Analysis Methods

The study selected 8 wooden chairs and measured the basic dimensions of their three-dimensional corner joints using a vernier caliper whose accuracy is 0.01 mm and rounding to a value without a comma, as shown in Table 1. The range of values for the mortise width and depth was determined using the ideal method and the optimized method. The maximum and minimum values were analyzed and, after rounding up, the kinds of (B_2, C_1) combinations before and after using the optimized method were compared. The margin parameters mainly concerned the calculation and analysis of the b_t , which has the most possible variations. Therefore, according to the different possible situations of B_{tm} , the study selected the minimum post width of case 1 and the maximum post width of case 8 in the axial direction of the cede tenon and the minimum post thickness of case 6 and case 1 with thickness greater than constant z in the beneficial tenon axis. Because no situations that meet (3b) were collected in the cases, a hypothetical case was set up ($T_m = T_t = 18$ mm) in the axial direction of the beneficial tenon. The b_t values for the above combinations were calculated and analyzed for at least three combinations of ($minB, minC$), ($minB, maxC$), and ($maxB, minC$).

Table 1. Cases' basic dimensions of three-dimensional corner joints.

Case	Rail (mm)		Post (mm)		Case	Rail (mm)		Post (mm)	
	T_t	W_m	T_m			T_t	W_m	T_m	
1	18	28	28	5	18	42	35		
2		30	30	6		50	22		
3		35	28	7		54	27		
4		36	36	8		58	28		

3. Results

3.1. Cases' Parameter Value in the Axial Direction of Cede Tenon

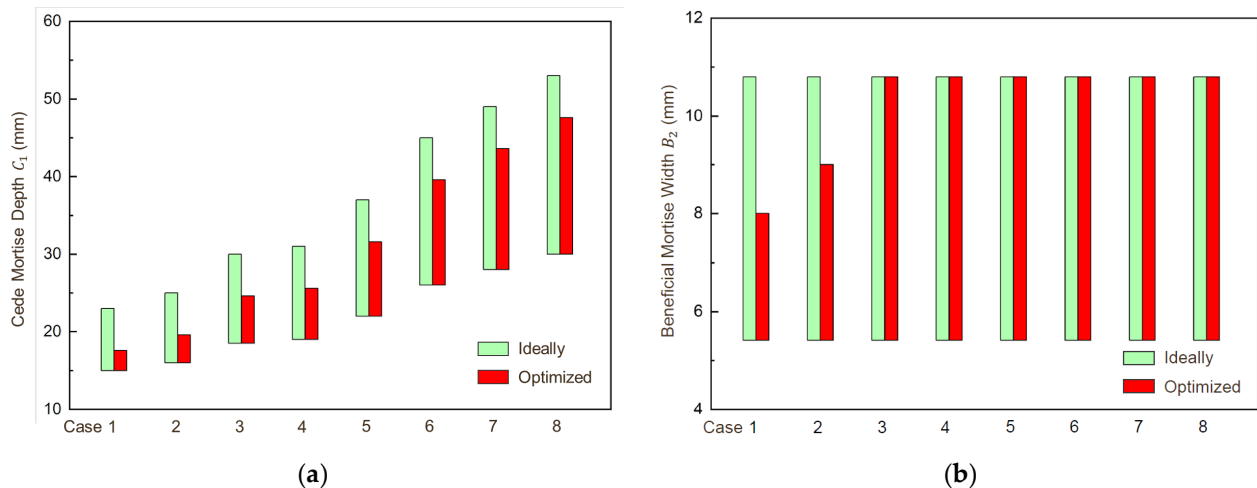
In the axial direction of the cede tenon, the limit values of the beneficial mortise width (B_2) and the cede mortise depth (C_1) parameters are first analyzed. As shown in Table 2, after using Formulas (4) and (5) for calculation, the $maxC_1$ for all cases decreased by 5.4 mm. The $minB_2$ and the $minC_1$ are consistent with the values calculated by Formula (1), and most of the $maxB_2$ values also match the results calculated by Formula (1). However, when the post width is smaller, the $maxB_2$'s value often decreases. When the post width is 28 mm and 30 mm, $maxB_2$ decreased by 2 mm and 1 mm, respectively. According to Formula (4), C_1 is particularly affected by the dimension of the post width, where the beneficial mortise width needs to occupy a certain dimension of the post width. Therefore, when the post width is small, both the minimum cede mortise depth ($minC_1$) and the maximum cede mortise depth ($maxC_1$) are restricted by the post width (W_m) and beneficial mortise width (B_2).

Table 2. Comparison of B_2 and C_1 limit values before optimization (ideally) and after optimization (optimized).

Case	Rail (mm)	Post (mm)	Mortise (Ideally) (mm)				Mortise (Optimized) (mm)			
	T_{t2}	W_m	$minB_2$	$maxB_2$	$minC_1$	$maxC_1$	$minB_2$	$maxB_2$	$minC_1$	$maxC_1$
1		28			15	23		8	15	17.6
2		30			16	25		9	16	19.6
3		35			18.5	30			18.5	24.6
4		36			19	31			19	25.6
5	18	42	5.4	10.8	22	37	5.4		22	31.6
6		50			26	45		10.8	26	39.6
7		54			28	49			28	43.6
8		58			30	53			30	47.6

According to [18,26], $z = 5$ and $\Delta C = 1$ were substituted to respective formulas for calculation. The value of z and ΔC can be set according to different wood species, drilling machines, etc.

Next, an analysis was conducted on the value range of the cede mortise depth (C_1) and beneficial mortise width (B_2) before and after optimization. As shown in Figure 6, the value range of C_1 for all cases has been reduced. Especially for the parts with smaller post widths, which are 28 mm and 30 mm, respectively, the optimized method can narrow the value range of C_1 to a narrower level. It is reduced from 15~23 mm and 16~25 mm to 15~17.6 mm and 16~19.6 mm, respectively. As for the value range of B_2 , only W_m values of 28 mm and 30 mm have been reduced, while others remain unchanged. Therefore, the parametric optimized method can obtain a more reasonable value range, especially when the post width is small.

**Figure 6.** Comparison of B_2 and C_1 value ranges before optimization (ideally) and after optimization (optimized). (a) Comparison of C_1 value range; (b) comparison of B_2 value range.

Based on optimizing the value range of the cede mortise depth (C_1) and the beneficial mortise width (B_2), (B_2, C_1) possible combinations of the cede tenon axis were further derived, as shown in Table 3. When B_2 is small, the C_1 can be larger, and vice versa. When C_1 is known, a more refined range of the other dimension can be quickly obtained, and vice versa. After obtaining the possible (B_2, C_1) combinations, the quantity of (B_2, C_1) before and after optimization was compared, as shown in Figure 7. Compared with the ideal (B_2, C_1) combinations, the quantity of optimized combinations for case 1 was reduced by 23, and the quantity of combinations for the other 7 cases was reduced by 24. When the post width ($W_m = 28$ mm) dimension is at the minimum value of 28 mm, the quantity of combinations

is only four. This is because, when the W_m is smaller, C_1 is limited by the other parameter dimensions in that axis to avoid structure conflict. Thus, regardless of the dimensions of the joints, the parametric optimized method of the cede tenon axis can stably reduce the quantity of (B_2, C_1) combinations, especially for three-dimensional corner joints with small post width dimensions, which can reduce the (B_2, C_1) combination quantity to a low level and facilitate selection of the appropriate values.

Table 3. (B_2, C_1) possible values.

Case	Rail (mm)	Post (mm)	(B_2, C_1) Possible Values (Optimized) (mm)		
	T_{t2}	W_m	$B_2 = 6$	$B_2 = 8$	$B_2 = 10$
1	18	28	$C_1 = 15\sim 17$	$C_1 = 15$	-
2		30	$C_1 = 16\sim 19$	$C_1 = 16\sim 17$	-
3		35	$C_1 = 19\sim 24$	$C_1 = 19\sim 22$	$C_1 = 19\sim 20$
4		36	$C_1 = 19\sim 25$	$C_1 = 19\sim 23$	$C_1 = 19\sim 21$
5		42	$C_1 = 22\sim 31$	$C_1 = 22\sim 29$	$C_1 = 22\sim 27$
6		50	$C_1 = 26\sim 39$	$C_1 = 26\sim 37$	$C_1 = 26\sim 35$
7		54	$C_1 = 28\sim 43$	$C_1 = 28\sim 41$	$C_1 = 28\sim 39$
8		58	$C_1 = 30\sim 47$	$C_1 = 30\sim 45$	$C_1 = 30\sim 43$

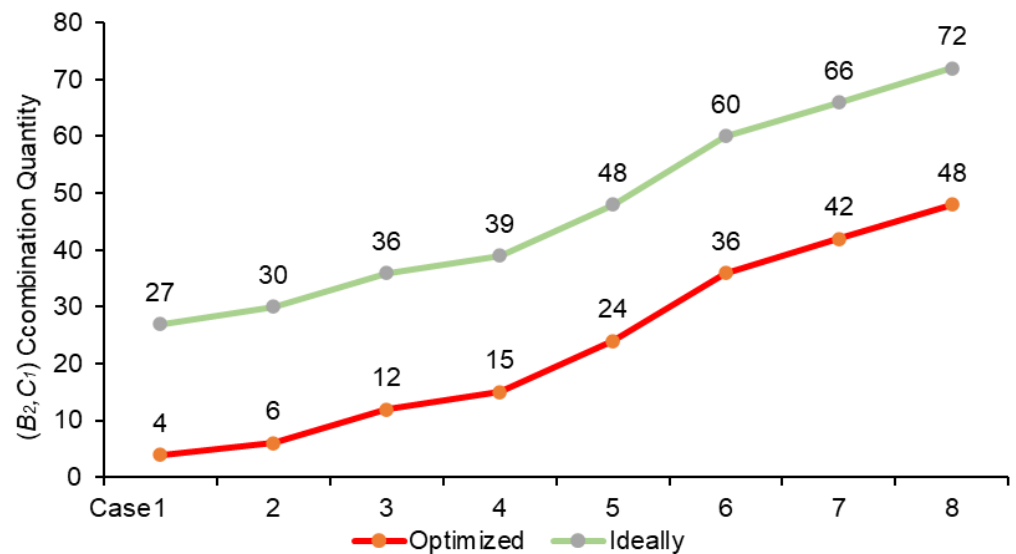


Figure 7. Comparison of (B_2, C_1) combination quantity before (ideally) and after optimization (optimized).

According to the possible different values of margin thickness from the rail₂ reference edge to the post reference edge (B_{tm2}), the values of margin thickness from the beneficial mortise–tenon to the rail₂ reference edge (b_{t2}) were analyzed by selecting cases of the smallest ($minW_m = 28$ mm) and largest ($maxW_m = 58$ mm) post width for the cede tenon axis, as shown in Table 4. If the before-optimization Formula (2c) is used for calculation, the maximum value range of b_{t2} should be 0–12 mm, and the quantity of available values is 13. After using the optimized Formula (6), considering all possible values of B_{tm2} , the range of available values for b_{t2} in case 1 is 0–7 mm, and when considering the value of B_{tm2} , the range of available values for b_{t2} is further narrowed, and the quantity of available values is reduced to at most three and at least one. This is because the minimum cede mortise depth ($minC_1$) and the minimum beneficial mortise width ($minB_2$) already occupy most of the post width values; the possible value range of B_{tm2} is narrowed, thus further narrowing the range of b_{t2} values. The available value range of b_{t2} for case 8 is 0–12 mm, consistent with

the ideal method, but when considering the value of B_{tm2} , the range of available values is further narrowed, with the quantity of available values ranging from 1 to 13. In summary, based on the data in Table 4 and Formulas (4)–(6), it can be seen that the width of the post and the thickness of the rail₂ will affect the values of the cede tenon axis mortise parameter combinations (B_2, C_1), which will further affect the values of B_{tm2} and the range of available values and quantity of b_{t2} 's available values.

Table 4. The optimized values of B_{tm2} and limit value of b_{t2} .

Case	T_{t2} (mm)	W_m (mm)	C_1 (mm)	B_2 (mm)	B_{tm2} (mm)	$minb_{t2}$ (mm)	$maxb_{t2}$ (mm)	b_{t2} Val. Qua.	Formula
1	18	28	15	6	0	5	7	3	(6b)
					5	0	2	3	(6c)
					7	0	0	1	(6d)
			17	8	0	5	5	1	(6b)
					5	0	0	1	(6c)
					0	5	5	1	(6b)
	18	18	30	6	0	0	12	13	(2c)
					22	0	0	1	(6a)
					0	0	8	9	(2c)
			41	10	18	0	0	1	(6a)
					0	5	11	7	(6b)
					5	0	6	7	(6c)
8	58	41	6	11	0	0	1	(6d)	
				0	5	7	3	(6b)	
				5	0	2	3	(6c)	
		47	10	7	0	0	1	(6d)	
				0	5	5	1	(6b)	
				5	0	0	1	(6c)	

The margin thickness parameter is defined as a non-negative integer.

3.2. Cases' Parameter Values in the Axial Direction of Beneficial Tenon

In the axial direction of the beneficial tenon, the limit values of the cede tenon width (B_1) and beneficial tenon depth (C_2) remain consistent with those of Formula (1) before optimization, as shown in Table 5.

Using the same analytical method as for b_{t2} , Formulas (2c) and (3) were used to calculate the value range and the quantity of values for margin thickness from beneficial mortise–tenon to the rail₁ reference edge (b_{t1}). Case 6 with the minimum post thickness, case 1 with a thickness greater than z , and a hypothetical case were chosen. Because no cases were found satisfying Formula (3b), a hypothetical case was also included (with $T_m = T_t = 18$ mm). As shown in Table 6, case 1's b_{t1} had an ideal value coverage range of 0–12 mm, with a minimum value quantity of 9 and a maximum value quantity of 13. For case 6, the range of values for b_{t1} was reduced from 0–12 mm to 1–11 mm using the optimized method, with a minimum value quantity of 3 and a maximum value quantity of 7. This indicates that when the thickness of the rail₁ (T_t) is not significantly different from that of the post thickness (T_m), the value range for b_{t1} is more accurate than that before optimization with Formula (2c), and the actual value range can be further narrowed based on the actual value of B_{tm1} . The range of values for b_{t1} was further reduced to 5–7 mm for the hypothetical case, with a minimum quantity of one value and a maximum quantity of

three values, indicating that when T_t equals T_m , the quantity of possible values for B_{tm1} decreases, and the range of values for b_{t1} subsequently decreases to a minimum level. In summary, the optimized method can further reduce the range of values for B_{tm1} , b_{t1} , and the quantity of possible values for b_{t1} when the difference between the post thickness and the rail₁ thickness is less than constant z , compared to the method before optimization.

Table 5. The limit values of B_1 , C_2 , and quantity of (B_1, C_2) combinations.

Case	Rail ₁ (mm)	Post (mm)	Mortise (mm)				(B_1, C_2) Qua.
	T_{t1}	T_m	$minB_1$	$maxB_1$	$minC_2$	$maxC_2$	
1	18	28	5.4	10.8	15	23	27
2		30			16	25	30
3		28			15	23	27
4		36			19	31	39
5		35			18.5	30	36
6		22			12	17	18
7		27			14.5	22	24
8		28			15	23	27

According to [18,26], $z = 5$ and $\Delta C = 1$ were substituted to respective formulas for calculation. The value of z and ΔC can be set according to different wood species, drilling machines, etc. Because there is no correlation between B_1 and C_2 in the beneficial tenon axis, the (B_1, C_2) combinations in this direction are the product of the quantity of B_1 and C_2 integral values.

Table 6. The optimized limit values of b_{t1} .

Case	T_{t1} (mm)	T_m (mm)	B_1 (mm)	B_{tm1} (mm)	$minb_{t1}$ (mm)	$maxb_{t1}$ (mm)	b_{t1} Val. Quan.	Formula	
1	18	28	6	0	0	12	13	(2c)	
				10	0	12	13		
				10	0	8	9		
6		22	6	0	5	11	7	(3a)	
				4	1	7	7		
				0	5	7	3		
Hypo.		18	10	10*	4	1	3	3	(3b)
					6	0	7	3	
	8				0	5	1		
				0	-	-	-	-	

* In the case of Hypothesis, when $B_1 = 10$ mm, $z = 5$ mm, b_{t1} 's value cannot be satisfied with Formula (3b).

4. Discussion

4.1. Effect of Three-Dimensional Corner Joint in Parameter Values

For three-dimensional corner joints of small dimensions, in the axial direction of the cede tenon, the minimum cede mortise depth and the minimum beneficial mortise width already occupy a large part of the width dimension of the post. Therefore, the range of values for the mortise–tenon margin parameter dimension is generally small, and the optimized method can limit the range of values for each margin parameter within a smaller range. In the axial direction of the beneficial tenon, the margin of the cede tenon can also be restricted to a more reasonable range. For three-dimensional corner joints of large dimensions, the range of values for each parameter in the cede tenon axis is generally wide.

However, the optimized range of values can still filter out impossible value intervals [27,28]. In the axial direction of the beneficial tenon, the optimized range of values is the same as the range calculated by the ideal method. Overall, the optimized method of the parameter range for three-dimensional corner joints has a good effect on the value range of parameters for small dimensions of three-dimensional corner joints.

4.2. Further Optimization for Parameter Values

Although the calculated parameter value ranges can be narrowed down in practical design and production, wide value ranges of the parameters can still cause problems for design and production. This is particularly true for the parameter in the beneficial tenon axis, where the parameter value ranges are mostly determined using the basic ideal method Formulas (1) and (2). Therefore, taking both processing and mechanical performance requirements into account, the value ranges of B_1 , B_{tm1} , and B_{t1} in the beneficial tenon axis can be set to the same values and combinations as in the cede tenon axial direction, to further narrow the dimensional parameter range and improve standardization [29–32]. As for mortise depth (C_1), current research indicates that the tenon length (tenon length plus fit parameters value ΔC equals mortise depth) has a significant impact on the mechanical performance. Therefore, the value range of C_1 can vary within a certain limit, and if a standard value is to be set, the overall structural safety requirements of the furniture should be taken into account [16,17,28,33]. In addition, for the optimization of all parameters, the following can be considered: (1) wood species (such as density and water content, etc.) and grain orientations for more accurate values; (2) wood parts' fundamental deviations and tolerance zones for woodworking and wood processing: by adding or subtracting from basic values, woodworking machines can be connected with joints for each parameter more accurately and quickly.

In the cases studied in this paper, the thicknesses of both rail₁ and rail₂ are the same, so their values for the mortise width are almost identical. In practical situations, even if the thicknesses of rail₁ and rail₂ differ slightly, if the constraints are met, the optimized method for the three-dimensional corner joint parameters can still be used. Subsequently, by analyzing the similarity of the attribute parameter in two axes, values can be comprehensively optimized based on mechanical performance requirements, shape requirements, and manufacturing requirements [34–40]. It should be noted that, for convenience in calculation and analysis, this study mainly describes the dimensions of the mortise, while the dimensions of the tenon can be calculated based on the dimensions of the mortise and the interference fit parameters (ΔB , ΔC).

5. Conclusions

This research adopts a parametric approach to develop an optimized method for the three-dimensional corner joints of wooden furniture, based on the ideal value range of mortise–tenon joints. Case studies were used to verify and analyze the optimized method. The method can quickly and effectively obtain reasonable value intervals for parameters while avoiding structure conflicts in both theoretical and practical applications [41–43]. The specific research results of this paper are as follows.

- (1) Based on the ideal value range of the mortise–tenon joint parameters, this study further derived parameter value optimized methods for the beneficial tenon axis and the cede tenon axis, which theoretically narrowed the coverage range of at least four main parameters: B_2 , C_1 , b_{t1} , and b_{t2} .
- (2) The analysis of the cases' data shows that in the axial direction of the cede tenon, the maximum depth of all cede mortises decreased by 5.4 mm, and the (B_2 , C_1) combination kinds decreased by at least 23. When the post width is 28 mm and 30 mm, the width of the beneficial mortise is reduced by 2 mm and 1 mm, respectively, compared with the ideal value, and the (B_2 , C_1) combination kinds are reduced to four and six, respectively. When the post width is smaller, the coverage range of b_{t2} is reduced from 0–12 mm with the ideal method to 0–5 mm with the optimized method, and

depending on the different values of B_{tm2} , the quantity of values can be reduced to a minimum of one and a maximum of three. When the post width is larger, the quantity of values that b_{t2} can take is reduced to a minimum of one. In the axial direction of the beneficial tenon, when B_{tm1} is less than constant z , the parameter value range and quantity of values of b_{t1} decrease as B_{tm1} decreases. Thus, the optimized method can significantly reduce the range of values in the cede tenon axis. The range of values in the beneficial tenon axis can also be reduced to a certain extent along with corresponding values, and the more dimension parameter setting values or standard values, the more the coverage range of dimension parameters will converge, and the fewer values will be required.

The parametric optimized method for wooden furniture three-dimensional corner joints can be applied to all wooden furniture with three-dimensional corner joints using rectangular or round-end mortise–tenon joints [44,45]. This method provides ideas for improving the digital and standardization level of wooden furniture structures. The application of this method should also consider wood species, grain orientations, wood parts' fundamental deviations and tolerance zones for woodworking and wood processing, etc., and carry on a simple calculation of each parameter, so as to more accurately and quickly connect all parameters to CNC woodworking machines. In further research, it is possible to study the comprehensive effects of single and multiple parameters on mechanical performance and processing efficiency and find the optimal standard values to improve the standardization of the furniture structure.

Author Contributions: Conceptualization, X.X. (Xiutong Xu) and X.X. (Xianqing Xiong); methodology, X.X. (Xiutong Xu) and X.X. (Xianqing Xiong); software, X.X. (Xiutong Xu) and X.Y.; validation, X.X. (Xiutong Xu) and X.Y.; formal analysis, X.X. (Xiutong Xu) and M.Z.; investigation, X.X. (Xiutong Xu); resources, X.X. (Xianqing Xiong) and M.Z.; data curation, X.X. (Xiutong Xu) and X.Y.; writing—original draft preparation, X.X. (Xiutong Xu); review and editing, X.X. (Xianqing Xiong), X.X. (Xiutong Xu), X.Y. and M.Z.; supervision, X.X. (Xianqing Xiong); funding acquisition, X.X. (Xianqing Xiong). All authors have read and agreed to the published version of the manuscript.

Funding: This research was funded by the National Key R&D Program of China (2018YFD0600304) and the Technology Innovation Alliance of Wood/Bamboo Industry (TIAWBI202010).

Data Availability Statement: Data are contained within the article.

Acknowledgments: The authors would like to thank Shiyuan Huang, a postgraduate student from the University of Macau, for her help in writing.

Conflicts of Interest: The authors declare no conflict of interest.

References

1. Xiong, X.Q.; Yue, X.Y. Research and application progress of home intelligent manufacturing technologies in China. *J. For. Eng.* **2022**, *7*, 26–34. [[CrossRef](#)]
2. Xiong, X.; Ma, Q.; Yuan, Y.; Wu, Z.; Zhang, M. Current situation and key manufacturing considerations of green furniture in China: A review. *J. Clean. Prod.* **2020**, *267*, 121957. [[CrossRef](#)]
3. Zhu, Z.; Jin, D.; Wu, Z.; Xu, W.; Yu, Y.; Guo, X.; Wang, X. Assessment of surface roughness in milling of beech using a response surface methodology and an adaptive network-based fuzzy inference system. *Machines* **2022**, *10*, 567. [[CrossRef](#)]
4. Li, R.; Zhao, S.; Yang, B. Research on the application status of machine vision technology in furniture manufacturing process. *Appl. Sci.* **2023**, *13*, 2434. [[CrossRef](#)]
5. Wu, Q.; Liu, F.; Hu, R.; Yu, H. Research on performance optimization method of mechanical parts based on CAD/CAE integration. *J. Mech. Strength* **2021**, *43*, 1504–1509. [[CrossRef](#)]
6. Xiong, X.; Yue, X.; Wu, Z. Current status and development trends of Chinese intelligent furniture industry. *J. Renew. Mater.* **2023**, *11*, 1353–1366. [[CrossRef](#)]
7. Fu, W.-L.; Guan, H.-Y. Numerical and theoretical analysis of the contact force of oval mortise and tenon joints concerning outdoor wooden furniture structure. *Wood Sci. Technol.* **2022**, *56*, 1205–1237. [[CrossRef](#)]
8. Lu, D.; Xiong, X.; Lu, G.; Gui, C.; Pang, X. Effects of NaOH/H₂O₂/Na₂SiO₃ bleaching pretreatment method on wood dyeing properties. *Coatings* **2023**, *13*, 233. [[CrossRef](#)]
9. Yu, M.; Sun, D.; Zou, W.; Wang, Z.; Jiang, X.; Yao, L.; Kong, J. Mechanical analysis of new Chinese style wood chairs using ANSYS. *J. For. Eng.* **2021**, *6*, 178–184. [[CrossRef](#)]

10. Xu, X.T.; Xiong, X.Q.; Zhang, Y.M.; Ren, G.J.; Cheng, Y.Q. Structural innovation and design improvement of detachable solid wood cabinet door with rectangular mortise and tenon joints. *Furniture* **2022**, *43*, 24–26+117.
11. Tang, L.; Lu, L.; Guan, H. Modern optimized design and anti-bending property of traditional corner joints. *J. For. Eng.* **2022**, *7*, 166–173. [[CrossRef](#)]
12. Tang, L.; Guan, H.; Wang, N.; Dai, P. Development of intelligent programming system for numerical controlled mortise and tenon joint. *J. Beijing For. Univ.* **2019**, *41*, 134–142. [[CrossRef](#)]
13. Yuan, Z.; Sun, C.; Wang, Y. Design for manufacture and assembly-oriented parametric design of prefabricated buildings. *Autom. Constr.* **2018**, *88*, 13–22. [[CrossRef](#)]
14. Geren, N.; Akçalı, O.O.; Bayramoğlu, M. Parametric design of automotive ball joint based on variable design methodology using knowledge and feature-based computer assisted 3D modelling. *Eng. Appl. Artif. Intell.* **2017**, *66*, 87–103. [[CrossRef](#)]
15. Liu, X.; Tang, L.; Yi, Y.; Ni, Z. Intelligent design based on holographic model using parametric design method. *J. Ambient Intell. Humaniz. Comput.* **2019**, *10*, 1241–1255. [[CrossRef](#)]
16. Kasal, A.; Smardzewski, J.; Kuşkun, T.; Erdil, Y.Z. Numerical analyses of various sizes of mortise and tenon furniture joints. *BioResources* **2016**, *11*, 6836–6853. [[CrossRef](#)]
17. Hu, W.; Chen, B. A methodology for optimizing tenon geometry dimensions of mortise-and-tenon joint wood products. *Forests* **2021**, *12*, 478. [[CrossRef](#)]
18. Guan, H. Modern furniture structures 1st chapter: Modern solid wood furniture structure—Joints and their requirements. *Furniture* **2007**, *155*, 54–59. [[CrossRef](#)]
19. Smardzewski, J. *Furniture Design*; Springer: Dordrecht, The Netherlands, 2015; Volume 6, pp. 226–249. [[CrossRef](#)]
20. Tang, L.; Guan, H. Intelligent method of determining dimension of mortise and tenon joint based on parameterization. *J. Beijing For. Univ.* **2021**, *43*, 143–154. [[CrossRef](#)]
21. Song, M.; Buck, D.; Yu, Y.; Du, X.; Guo, X.; Wang, J.; Zhu, Z. Effects of Tool Tooth Number and Cutting Parameters on Milling Performance for Bamboo–Plastic Composite. *Forests* **2023**, *14*, 433. [[CrossRef](#)]
22. Lee, I.-J. Using augmented reality to train students to visualize three-dimensional drawings of mortise–tenon joints in furniture carpentry. *Interact. Learn. Environ.* **2020**, *28*, 930–944. [[CrossRef](#)]
23. Chen, B.; Xia, H.; Hu, W. The design and evaluation of three-dimensional corner joints used in wooden furniture frames: Experimental and numerical. *BioResources* **2022**, *17*, 2143–2156. [[CrossRef](#)]
24. Xiong, X.Q.; Ren, J. Digital design technology of furnishing products in intelligent manufacturing. *Chin. J. Wood Sci. Technol.* **2021**, *35*, 14–19. [[CrossRef](#)]
25. Rempling, R.; Mathern, A.; Ramos, D.T.; Fernández, S.L. Automatic structural design by a set-based parametric design method. *Autom. Constr.* **2019**, *108*, 102936. [[CrossRef](#)]
26. Guan, H. Modern furniture structures 2nd chapter: Modern solid wood furniture structure—structures in details and on the whole. *Furniture* **2007**, *156*, 45–51. [[CrossRef](#)]
27. Chen, B.; Guan, H. A novel method and validation for obtaining the optimal interference fit of round-end mortise-and-tenon joint. *Wood Mater. Sci. Eng.* **2023**, 1–11. [[CrossRef](#)]
28. Hu, W.; Liu, N.; Guan, H. Experimental and numerical study on methods of testing withdrawal resistance of mortise-and-tenon joint for wood products. *Forests* **2020**, *11*, 280. [[CrossRef](#)]
29. Wang, Y.; Chen, J.; Fang, Z.; Wang, H. Status review of wooden furniture standardization in China. *Chin. J. Wood Sci. Technol.* **2021**, *35*, 73–78. [[CrossRef](#)]
30. Xiong, X.Q.; Ma, Q.R.; Yuan, Y.Y.; Pan, Y.T.; Niu, Y.T. Digital design and manufacturing of furniture enterprises oriented to intelligent manufacturing. *J. For. Eng.* **2020**, *5*, 174–180. [[CrossRef](#)]
31. Zhang, T.; Hu, W. Numerical study on effects of tenon sizes on withdrawal load capacity of mortise and tenon joint. *Wood Res.* **2021**, *66*, 321–330. [[CrossRef](#)]
32. Xu, X.T.; Yan, X.X. Study on and probe into national standards of children’s furniture structural safety. *For. Mach. Woodwork. Equip.* **2021**, *49*, 43–46. [[CrossRef](#)]
33. Xu, J.; Zhu, X.; He, R.; Ren, H.; Li, J. Optimization of oval mortise and tenon joint based on group technology. *J. For. Eng.* **2017**, *2*, 144–149. [[CrossRef](#)]
34. Hitka, M.; Štarchoň, P.; Šimanová, L.; Čuta, M.; Sydor, M. Dimensional solution of wooden chairs for the adult bariatric population of slovakia: Observational study. *Forests* **2022**, *13*, 2025. [[CrossRef](#)]
35. Gao, L.; Xu, W.; Li, R.; Huang, Q. Influencing factors of t-type parts joint strength of ellipse mortise and tenon. *China For. Prod. Ind.* **2019**, *50*, 19–22. [[CrossRef](#)]
36. Smardzewski, J. Strength of profile-adhesive joints. *Wood Sci. Technol.* **2002**, *36*, 173–183. [[CrossRef](#)]
37. Zhu, Z.; Buck, D.; Wang, J.; Wu, Z.; Xu, W.; Guo, X. Machinability of different wood-plastic composites during peripheral milling. *Materials* **2022**, *15*, 1303. [[CrossRef](#)]
38. Li, R.; He, C.; Xu, W.; Wang, X.A. Prediction of surface roughness of CO2 laser modified poplar wood via response surface methodology. *Maderas. Cienc. Tecnol.* **2022**, *24*, 1–12. [[CrossRef](#)]
39. Peng, W.; Yan, X. Preparation of tung oil microcapsule and its effect on wood surface coating. *Polymers* **2022**, *14*, 1536. [[CrossRef](#)]
40. Yan, X.; Peng, W.; Qian, X. Effect of water-based acrylic acid microcapsules on the properties of paint film for furniture surface. *Appl. Sci.* **2021**, *11*, 7586. [[CrossRef](#)]

41. Lin, T. Preliminary study on the parametric manufacturing process of traditional woodworking tenon. *ICFXD* **2021**, *1*, 140501–140511. [[CrossRef](#)]
42. Gao, L.; Xu, W.; Wu, S.; Zhan, X.; Shen, Z. Research on the optimization of the mortise and tenon connection of solid wood furniture components. *Furniture* **2018**, *39*, 4–7. [[CrossRef](#)]
43. Yi, L.; He, J.; Zhang, Z.; Zhang, J. Construction of digital model of round-backed using NX software and MBD technology. *J. For. Eng.* **2023**, *8*, 180–186. [[CrossRef](#)]
44. Ren, J.; Xiong, X.Q. Digital design process and part family division of solid wood custom cabinet door based on multi-attribute overlapping clustering technology. *BioResources* **2020**, *17*, 5393. [[CrossRef](#)]
45. Langová, N.; Réh, R.; Igaz, R.; Krišťák, L.; Hitka, M.; Joščák, P. Construction of wood-based lamella for increased load on seating furniture. *Forests* **2019**, *10*, 525. [[CrossRef](#)]

Disclaimer/Publisher’s Note: The statements, opinions and data contained in all publications are solely those of the individual author(s) and contributor(s) and not of MDPI and/or the editor(s). MDPI and/or the editor(s) disclaim responsibility for any injury to people or property resulting from any ideas, methods, instructions or products referred to in the content.